GEOPHYSICAL RESEARCH LETTERS, VOL. 14, NO. 5, PAGES 542-545, MAY 1987

WAVEFORM EFFECTS OF A HIGH-VELOCITY, SUBDUCTED SLAB

John E. Vidale

Richter Seismological Laboratory, University of California, Santa Cruz, CA 94065

Abstract. Creager and Jordan [1986] propose that penetration of subducting slabs under the Kurile Islands and other subduction zones to depths of at least 1000 km is necessary to explain travel time anomalies of deep earthquakes. Such penetration would also be expected to affect the amplitudes and waveforms of the body waves from earthquakes. Synthetic seismograms appropriate for a record section in a plane perpendicular to the strike of the slab are presented using a coupled finite-difference and Kirchhoff method. Our shear-wave version of the compressional-wave velocity structure of Creager and Jordan [1986] produces an amplitude decrease up to a factor of four and waveform broadening up to 20 seconds for SH arrivals with a take-off angle pointing straight down the slab. Slabs that extend only 300 km below the earthquake but are half as thick and twice as anomalously fast as Creager and Jordan's [1986] velocity model will roughly preserve the travel time variation pattern, and show less waveform broadening, but produce first arrivals that are emergent. Slabs that become thicker with depth show less waveform broadening. Reconciliation of the amplitude, waveform distortion, and timing of body waves from deep events is necessary to understand the geometry of slabs in the upper mantle and near and below the 650 km discontinuity.

Introduction

The question of whether subducting slabs penetrate the 650 km discontinuity is of great concern to earth scientists. The most plausible theories of mantle convection have as end members the entire mantle overturning in a single layer of convection and two or more chemically distinct layers of mantle convection separated by a boundary near 650 km depth. To discriminate between these theories, research has been done with flow models, geoid observations, and inversions for mantle velocity models. The most detailed ideas about the geometry of slabs near and below the 650 km discontinuity are emerging from the study of travel time anomalies from deep earthquakes [Jordan, 1977, Creager and Jordan, 1984, 1986]. Using shear [Jordan, 1977] and compressional [Creager and Jordan, 1984, and Creager and Jordan, 1986] wave travel time anomalies as data, and models in which only temperature and the olivine - β spinel phase changes affect velocity to constrain the geometry of the slabs, the slabs are proposed to extend to a depths greater than 1000 km.

Although these studies use only travel time data to constrain velocity models of subducting slabs, the models have implications for amplitude and waveform effects of the deep slabs. With faster computers and more advanced finite difference methods [Vidale and Helmberger, 1986, and Vidale and Helmberger, 1987], these effects can be calculated. In this paper, I show that slab structures can produce noticeable distortions of the amplitudes and waveforms for teleseismic signals from deep earthquakes. It is important to be able to calculate the distortions due to a given slab structure, both to test hypotheses about slab structure and mineralogy and to separate the effects of slab geometry from the effects of other lateral velocity variations in the mantle, anisotropy, deformation of the 650 km discontinuity and the possible effect of structure at the core-mantle boundary. It is important to realize that a high-velocity slab is an anti-waveguide. Waves are continuously refracted out of the slab, leading to waveform distortion and a reduction in amplitude.

Paper number 7L7137.
0094-8276/87/007L-7137$03.00

Methods

We simulate the teleseismic signals of earthquakes in slabs using a sequence of methods. A fourth order 2-D acoustic (for P waves) or SH (for S waves) finite difference (FD) scheme is used in the vicinity of the slab. The source is isotropic in both the acoustic and the SH case, to keep the interpretation as simple as possible. Within the FD grid, the seismic energy interacts with the high-velocity slab. Although the seismograms may be calculated within the FD grid for distances up to 2000 km from the source, the waveforms may evolve further traveling to teleseismic distances. To propagate energy to distances greater than 2000 km, we first record the motions on a surface within the FD grid. From this surface, the seismic energy is propagated by a Kirchhoff scheme through a halfspace to a receiver 10,000 km from the source to allow the waveform to heal. Finally, the line source seismograms are transformed to point source seismograms by the line-to-point source mapping of Vidale and Helmberger [1987].

The source in this paper is placed at 515 km depth in the middle of the high-velocity slab. The FD grid covers an area from 400 to 1400 km depth and is 1600 km wide. The simulated teleseismic signals, then, are appropriate for energy that stays in the plane perpendicular to the strike of the subducting slab. Preliminary analysis of P-wave data on long-period WWSSN instruments [Vidale and Helmberger, 1986] and the broadband Graefenberg array [Engdahl and Kind, 1986], suggests that systematic slab-induced distortions for earthquakes and explosions at less than 200 km depth are most prominent for raypaths that travel directly down-dip from the source. Silver and Chan [1986], who examine S-waves on GDSN records from deeper sources, notice more distortion for arrivals that travel parallel to the strike of the slab. As the computation of synthetic seismograms is simpler perpendicular to the slab and there are systematic effects observed in this direction, there is much to be learned by the modeling techniques used in this paper.

Several complexities are ignored. Ray bending after the seismic signal leaves the FD grid is not included; similarly interactions with the CMB and any triplications due to gradients outside the FD grid are not included in this analysis. I wish to isolate the effects of the slab, however, and these other effects may be included later by WKB methods, for example, once we understand the effects of the slabs.

Discussion

Consider how a subducting slab might act as a waveguide, or, more accurately, as an anti-waveguide. A simple, but extreme model of a slab surrounded by warmer and therefore slower mantle material is a 80 km thick layer with compressional wave velocity of 10 km/sec surrounded on either side by two halfspaces with a velocity of 9 km/sec. The results of the FD method coupled with Kirchhoff method are shown in Figure 1.

The effects of a high-velocity layer at teleseismic distances

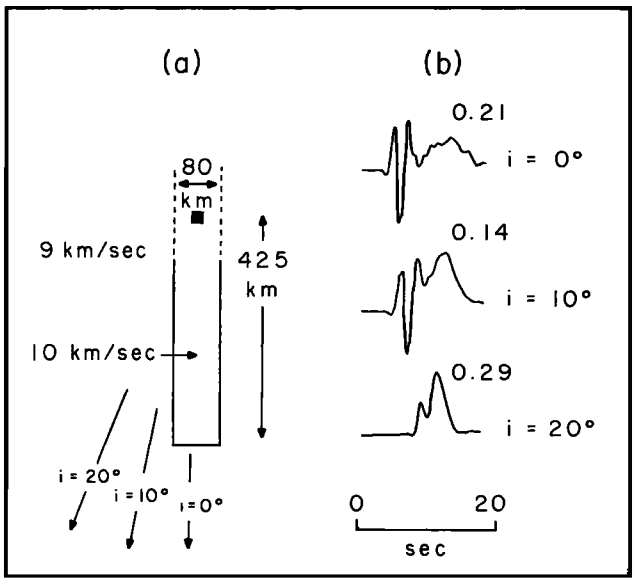

Fig. 1. Synthetic P-waves distorted by propagation through a high velocity, isotropic slab. The model is shown in Figure 1a, with the source indicated by a filled square. The receivers do not appear on this scale, but are in the direction indicated by the arrows at 0°, 10° and 20°. At small take-off angles, both the high-frequency, geometrical arrival and the non-geometrical lower-frequency arrival are visible. The amplitudes relative to the P-waves for a whole-space are printed above each trace.

may be seen in Figure 1. For the case of a receiver directly below a source (i = 0°) in a slab, the initial arrivals with a take-off angle near the vertical dip angle of the slab have a reduced amplitude and an earlier arrival time than if the slab had not been present. The earlier arrival time is, of course, due to passage through higher-velocity material. There are two mechanisms for amplitude loss in propagation down a high-velocity slab. The first mechanism, which is acting in this example, is diffraction out of the slab. Since the velocity in the slab is faster than velocity in the surrounding material, the wavefront in the slab becomes separated from the wavefront in the surrounding material. A sharp break in a seismic wavefront will tend to smear out as the wave propagates; this process may also be thought of as the break in the wavefront acting as a secondary source. The energy in the slab is then being drained out into the surrounding material as a diffracted wavefront. The longer the period of the energy, the more of the slab is within a wavelength or two of the edge of the slab, and the diffraction more rapidly drains the energy out into the surrounding medium. This process cannot be simulated with only geometrical rays.

The second mechanism can be calculated with a ray-tracing scheme; amplitude loss can occur through defocusing as indicated by the divergence of geometric rays. This mechanism does not act here because the bottom of the slab is flat. If the source were high-frequency enough, there would be no significant decay in amplitude in this case, at least for rays that travel down the geometric center of the slab. Conversely, if the bottom of the slab had been curved, then the high frequency energy would lose energy due to defocusing.

The longer-period pulse about 8 sec behind the first arrival in the seismograms in Figure 1 results from long-period energy that travels in the slower surrounding media and must diffract around the slab to reach the receiver. The second arrival has no analogue in the case where there is no slab. This pulse is not a geometrical arrival; this is clear if one considers the case of an infinitely thin, fast layer. The first, geometrical arrival will travel within the layer for some distance, but will have an infinitely small amplitude. Finite frequencies will act as if the infinitely thin layer does not exist.

As the take-off angle increases, the high-frequency arrival loses amplitude and precedes the second arrival by less time. At just past 20°, the two arrivals merge as the energy that travels down the fast slab no longer precedes the energy that travels straight from the source to the receiver. At take-off angles greater than 25°, there is little in the seismograms to indicate even the presence of a fast slab.

Figure 1 serves primarily to show the range of effects of a high-velocity slab; a more realistic structure is necessary to learn the effects we might expect to see in the Earth. The P-wave velocity model for the subducting slab in the Kurile-Kamchatka subduction zone for the depth range 400-1400 km taken from Creager and Jordan [1986] is shown in Figure 2. Creager and Jordan [1984] show much larger velocity anomalies for the slabs, but these results arise from errors in ray tracing [pers. comm., Creager, 1986]. The results for the FD-Kirchhoff scheme are also shown in Figure 2. The travel times are up to 3 sec early. The amplitudes for seismic energy with a take-off angle directly down the slab are reduced by a factor of 2 relative to the case with no anomalous slab. The waveform is broadened by up to 5 sec by interaction with the fast slab.

This amount of distortion may be noticeable in the data, but the distortions in the S-waves are likely to be greater. Observations on mineral samples show that temperature induced relative changes in shear velocity are about the same as relative changes in compressional velocity. On the other hand, lateral velocity variations in the mantle generally show

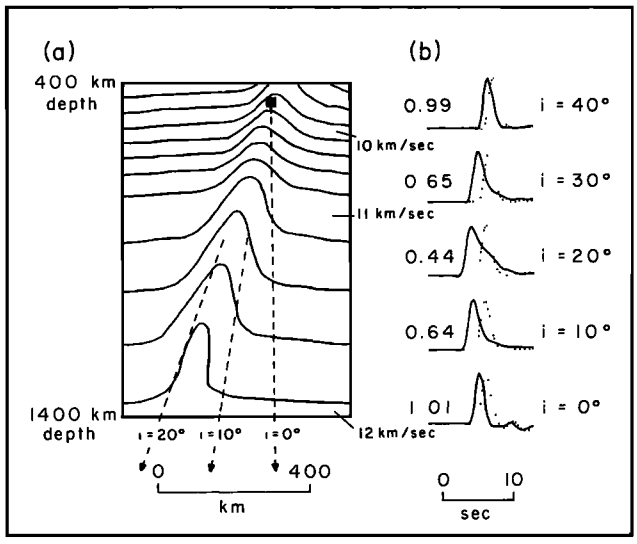

Fig. 2. Synthetic P-waves distorted by propagation through a thermal model of the P-wave velocity structure of subducting slabs. This model is taken from Creager and Jordan [1986] for the slab in the Kurile-Kamchatka subduction zone. The seismograms are computed at a range of 10,000 km for take-off angles ranging from 0° to 40°. The dotted seismograms are calculated from a model with no slab velocity anomaly. Printed above each trace is the amplitude ratio of the seismograms affected by the slab to the seismograms with no slab.

$\delta \ln V_s$ about $2\delta \ln V_p$ [e.g., Doyle and Hales, 1967, Anderson, 1986]. A common physical explanation is that the shear modulus varies much more than the bulk modulus. If lateral velocity variations are primarily due to changes in the shear modulus, the percentage variation in S-wave velocity would be about twice that of the P-wave velocity.

I construct the S-wave velocity structure of the slab by multiplying the percentage anomaly from Creager and Jordan's [1986] model shown in Figure 2a by 9/4 and superimposing this on the mantle structure from PREM [Dziewonski and Anderson, 1981]. The result is shown in Figure 3a. Several alternative geometries for slabs have also been proposed. Hager [1986] finds that if the lower mantle has a viscosity 100 times larger than the upper mantle, the slab flares outward as it sinks into the lower mantle. A simple flaring model is shown in Figure 3b, where at 1200 km depth, the slab has a width of about 500 km rather than 200 km as in Figure 3a. Creager and Jordan suggest that a 500 km width is less likely than a 200 km width, however, the sensitivity of travel time anomalies to the width of the slab is not well-established.

Jeanloz and Knittle [1986] and others argue that layered convection is occurring. If there is a large enough intrinsic density contrast between the upper and lower mantle, the slabs cannot penetrate the lower mantle as is indicated by the geometries in Figures 3a and 3b. If they did, the upper and lower mantles would be thoroughly mixed by now. The smoothed results from Creager and Jordan [1986] match well the smoothed pattern of travel time anomalies, so if slabs only extend to 650 km, the velocity anomalies must be stronger than indicated in Figure 3a to produce the same amount of travel time anomaly from a shorter travel path in the anomalous slab. Anderson [1986] finds that it is likely that the slab is composed of ilmenite minerals (the cold, high-pressure forms of enstatite, diopside, and garnet) below 400 km depth, which would be 10-20% faster than the surrounding mantle. Also, the short slab would have to be thinner than the long slab to produce even approximately the same residual sphere, at least in the isotropic case. Figure 3c shows such a short, thin and anomalously fast slab.

The seismograms from the models in Figure 3a, 3b, and 3c are shown in Figures 4a, 4b, and 4c. The "trim" slab derived from Creager and Jordan's [1986] model strongly affects the seismograms. The amplitude of the traces where the take-off angle is straight down the slab are a factor of three lower than for the case with no slab. The waveforms are broadened up to 20 sec by the non-geometrical arrival late in the record. The flaring slab also produces an long-

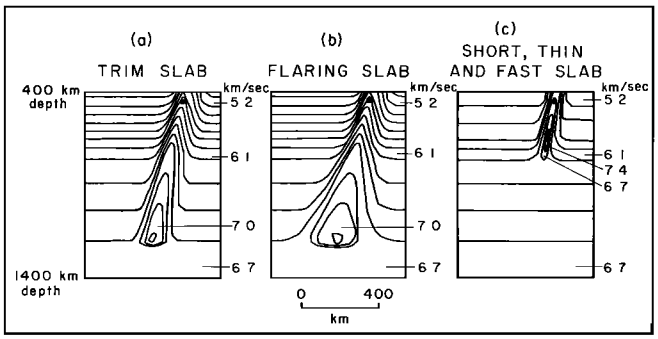

Fig. 3. Possible isotropic S-wave velocity structures for subducting slabs. Figure 3a shows a structure similar to Figure 2a, but with twice the percentage anomaly as the P-wave slab model. Figure 3b shows a model of a slab that flares out as it sinks deeper in the lower mantle. Figure 3c shows a slab that ends at 700 km depth, but has a 20% velocity anomaly in its center. This short, fast slab is also only half as wide as the slab in Figure 3a.

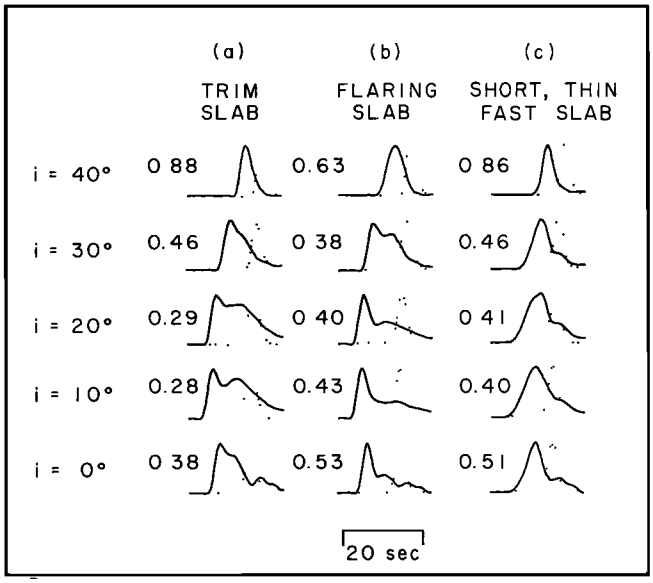

Fig. 4. SH waves distorted by propagation through the 3 models of the S-wave velocity structure shown in Figure 3. The SH waves are computed at a range of 10,000 km for take-off angles ranging from 10° to 40°. The dotted SH waves are calculated from a model with no slab velocity anomaly. Printed above each trace is the amplitude ratio of the SH waves affected by the slab to the SH waves with no slab. The take-off angle of i = 20° corresponds to rays taking off directly down dip.

period bump, though of smaller amplitude than the trim slab. The amplitude anomaly is still a factor of 2.5 for the flaring slab. The thin slab has such a narrow wave guide that the arrival begins gradually and even the upswing is broadened. The amplitude anomaly is again a factor of 2.5, and the broadening is again up to 10 secs.

These results suggest that the anomalous effects of the slab would be spread over a range of 20–30° in take-off angle. A careful analysis of Figure 4 shows that, as one expects, the flared slab produces a wider band of fast arrivals than the trim slab. The figure also suggests, however, that the best discriminant between the slab models is the waveform and amplitude data. S-waves may determine slab structure better than P-waves because the S-wave velocity anomalies are probably larger, as mentioned above. P-waves, however, have the advantage that Q has less effect.

Broadening of the S-wave displacement pulses of up to 20 sec has been observed for seismic signals from deep earthquakes by Silver and Chan [1986]. His observations have an azimuth and range that suggest the seismic energy took off from the source along the slab. Silver and Chan's [1986] data varies more rapidly with takeoff angle than the synthetic seismograms generated in this paper, suggesting that his broadened waveforms are the result of some structure farther from the earthquakes. Beck and Lay [1986] examined numerous S and ScS records from deep earthquakes at various azimuths and failed to see a strong systematic pattern of waveform broadening.

Conclusions

The effects on waveform and amplitude of competing isotropic models for the velocity structure in the area of subducting slabs may be calculated. The anomalous features of these models are of an observable magnitude.

The anomalous features are of three kinds. First, the faster material in the slab advances the arrivals that leave the

source region in the plane of the slab, as has been noted previously [e.g. Sleep, 1973, Jordan, 1977]. This feature can be most easily investigated by ray-tracing. Second, the faster material in the slab tends to defocus energy leaving the source region in the plane of the slab. This anomaly can also be investigated by ray-tracing, although smooth models would be required and the results from standard ray-tracing are only correct for infinite frequency. Third, the waveforms of energy that leaves the source region in this direction can be distorted, with emergent first arrivals and long-period, late diffracted arrival, which can make the full waveform appear as a broadened pulse rather than simply the source time function convolved with a Q operator as it would if there were no structure. Some type of full wave theory is required to properly reproduce these effects.

We have developed a scheme that combines an FD algorithm with a Kirchhoff surface, and can properly treat all three of the above features. We do not address the travel time anomalies, as they are investigated elsewhere [Creager and Jordan, 1986]. In general, thinner slabs of a given length produce more waveform broadening and smaller amplitudes for signals that leave the source region in the plane of the slab. Amplitude anomalies are more sensitive to details in the structure, but, for the structures used in this note, are large enough to be observable.

Reconciliation of the amplitude, waveform distortion, and timing of body waves from deep events is necessary to understand the geometry of slabs near and below the 650 km discontinuity.

Acknowledgements. This work was partly supported by Air Force-Cambridge grant F19628-83-K-0010. J.E.V. was supported by an NSF fellowship. I thank Don L. Anderson, Ken Creager, Don Helmberger, Heidi Houston, and Thorne Lay for discussions. Richard Stead provided the Kirchhoff program used. Don L. Anderson, Heidi Houston and Lorraine Hwang reviewed the manuscript. Contribution number 4408 from the Division of Geological and Planetary Sciences, California Institute of Technology, Pasadena, California, 91125.

References

Anderson, Don L., The mineralogy of deep slabs (abstract), *EOS Trans. AGU, 67*, 379, 1986.

Beck, S.L., and T. Lay, Test of the lower mantle slab penetration hypothesis using broadband S waves, *Geophys. Res. Lett., 10*, 1007-1010, 1986.

Creager, K.C. and T.H. Jordan, Slab penetration into the lower mantle, *J. Geophys. Res., 89*, 3031-3049, 1984.

Creager, K.C. and T.H. Jordan, Slab penetration into the lower mantle beneath the Mariana and other island arcs of the Northwest Pacific, *J. Geophys. Res., 91*, 3573-3589, 1986.

Dziewonski, A.M. and D.L. Anderson, Preliminary reference Earth model, *Phys. Earth Planet. Int., 25*, 297-356, 1981.

Engdahl, E.R. and R. Kind, Interpretation of broadband seismograms from central Aleutian earthquakes, *Annales Geophysicae, 4*, 233-240, 1986.

Hager, B.H., Fluid dynamics of the 670 discontinuity, *EOS Trans. AGU, 67*, 381, 1986.

Jeanloz, R. and E. Knittle, Reduction of mantle and core properties to a standard state by Adiabatic decompression, in *Chemistry and Physics of Terrestrial Planets*, S.K. Saxena, ed., Springer-Verlag, New York, pp. 275-309, 1986.

Jordan, T.H., Lithospheric slab penetration into the lower mantle beneath the sea of Okhotsk, *J. Geophys., 43*, 473-496, 1977.

Silver, P., and W. Chan, Observations of body wave multipathing from broadband seismograms: evidence for lower mantle slab penetration beneath the sea of Okhotsk, *J. Geophys. Res., 91*, 13787-13802, 1986.

Sleep, N.H., Teleseismic P-wave transmission through slabs, *Bull. Seismo. Soc. Am., 63*, 1349-1373, 1973.

Vidale, J.E. and D.H. Helmberger, Waveform effects of high-velocity, subducting slabs, *EOS Trans. AGU, 68*, 1114, 1986.

Vidale, J.E. and D.H. Helmberger, Path effects in strong motion seismology, chapter in volume of *Methods of Computational Physics*, Bruce Bolt, ed., 1987.

J. Vidale, Richter Seismological Laboratory, University of California, Santa Cruz, CA 95064.

(Received February 20, 1987;
accepted February 20, 1987.)